SCIENTIFIC REPORTS

OPEN

SUBJECT AREAS:
CANCER MICROENVIRONMENT
COLON CANCER

Received
25 July 2013

Accepted
18 September 2013

Published
8 October 2013

Correspondence and requests for materials should be addressed to C.J. (Christian.Jobin@medicine.ufl.edu)

VSL#3 probiotic modifies mucosal microbial composition but does not reduce colitis-associated colorectal cancer

Janelle C. Arthur[1], Raad Z. Gharaibeh[4], Joshua M. Uronis[1], Ernesto Perez-Chanona[2], Wei Sha[4], Sarah Tomkovich[3], Marcus Mühlbauer[1], Anthony A. Fodor[5] & Christian Jobin[1,2,3,6,7]

[1]Department of Medicine, [2]Pharmacology, [3]Microbiology and Immunology, University of North Carolina at Chapel Hill, Chapel Hill, NC 27599, USA, [4]Bioinformatics Services Division, Department of Bioinformatics and Genomics, University of North Carolina at Charlotte, Kannapolis, NC 28081, USA, [5]Department of Bioinformatics and Genomics, University of North Carolina at Charlotte, Charlotte, NC 28223, USA, [6]Department of Medicine, University of Florida at Gainesville, Gainesville, FL32611, USA, [7]Department of Infectious Diseases and Pathology, University of Florida at Gainesville, Gainesville, FL32611, USA.

Although probiotics have shown success in preventing the development of experimental colitis-associated colorectal cancer (CRC), beneficial effects of interventional treatment are relatively unknown. Here we show that interventional treatment with VSL#3 probiotic alters the luminal and mucosally-adherent microbiota, but does not protect against inflammation or tumorigenesis in the azoxymethane (AOM)/*Il10*$^{-/-}$ mouse model of colitis-associated CRC. VSL#3 (10^9 CFU/animal/day) significantly enhanced tumor penetrance, multiplicity, histologic dysplasia scores, and adenocarcinoma invasion relative to VSL#3-untreated mice. Illumina 16S sequencing demonstrated that VSL#3 significantly decreased (16-fold) the abundance of a bacterial taxon assigned to genus *Clostridium* in the mucosally-adherent microbiota. Mediation analysis by linear models suggested that this taxon was a contributing factor to increased tumorigenesis in VSL#3-fed mice. We conclude that VSL#3 interventional therapy can alter microbial community composition and enhance tumorigenesis in the AOM/*Il10*$^{-/-}$ model.

Millions of individuals worldwide consume probiotic bacteria with the goal of improving gastrointestinal (GI) health by restoring microbial homeostasis[1]. This is especially apparent among inflammatory bowel disease (IBD) patients, totaling an estimated 1.4 million Americans and 2.2 million Europeans, who have a high risk of developing colorectal cancer (CRC)[2,3]. Animal models and human clinical trials indicate that probiotics may reduce inflammation and alleviate symptoms of IBD[4], and it is tantalizing to consider that beneficial effects may also extend to CRC. The majority of probiotic research has centered around effects on the mammalian host with less emphasis on exploring the impact of probiotics on commensal microbes inhabiting the GI tract, commonly referred to as the gut microbiota.

The gut microbiota is a population of an estimated 100 trillions of microbes that reside within the GI tract and participate in a symbiotic relationship with their mammalian host. This population of microbes harbors 100-fold more genes than are found in the human genome, and its enzymatic capacity rivals that of the human liver[5]. Alteration in the composition of the gut microbiota, termed intestinal dysbiosis, is now regarded as a driving force behind the pathogenic features of IBD and appears to similarly impact the development of CRC[6–8]. Culture-independent rRNA sequence analyses have revealed differences in community composition of the luminal and mucosally-adherent microbiota between human IBD patients and healthy controls[9,10]. Similar analyses on human CRC patients have revealed significant differences in the luminal microbiota of cases vs. controls[1,11], and differences in microbial community composition and richness in healthy rectal tissue from patients with adenomas versus healthy controls[2,12–14]. Although it remains unclear which specific microbial taxa promote development of inflammation and CRC, several bacterial groups have been consistently identified as altered in these disease states. Bacteroidetes, a dominant phylum of the gut microbiota, were found to be less abundant in the tissue of adenoma-bearing patients and human colorectal tumors relative to that of healthy controls[4,13,15]. Proteobacteria, in contrast,

have been detected at increased abundance in human CRC tissue[5,12,13,16], tissue from IBD patients[6–8,17,18], and in mouse models of colitis and CRC[8–10,19].

VSL#3 is a commercially available probiotic cocktail (Sigma-Tau Pharmaceuticals, Inc.) of eight strains of lactic acid-producing bacteria: *Lactobacillus plantarum, Lactobacillus delbrueckii* subsp. *Bulgaricus, Lactobacillus paracasei, Lactobacillus acidophilus, Bifidobacterium breve, Bifidobacterium longum, Bifidobacterium infantis*, and *Streptococcus salivarius* subsp. *Thermophilus*. Orally administered VSL#3 has shown success in ameliorating symptoms and reducing inflammation in human pouchitis[20,21] and ulcerative colitis[22,23]. Preventive VSL#3 administration can also attenuate colitis in *Il10*$^{-/-}$ mice[24] and ileitis in SAMP1/YitFc mice[25]. Nonetheless, several reports indicate no beneficial effects of VSL#3 on murine dextran sulfate sodium (DSS) colitis[26], established ileitis in TNF$^{\Delta ARE/+}$ mice[27], or human pouchitis[28]. The mechanisms underlying the beneficial functions of VSL#3 are not well understood, but likely involve direct effects of probiotic activity on the mammalian host as well as indirect effects by altering the population dynamics of the gut microbiota as a whole. Indeed, pre-treatment with VSL#3 altered community composition, prevented DSS colitis, and diminished adenoma and adenocarcinoma formation in the AOM/DSS model[29,30]. In the rat TNBS model of inflammation-associated CRC, early administration of VSL#3 altered microbial diversity and delayed the transition from inflammation to dysplasia[31,32]. Thus it is clear that VSL#3 probiotic has the capability to prevent inflammation and carcinogenesis when used as a preventative strategy. However, the therapeutic potential of VSL#3 probiotic administered after the onset of inflammation remains unknown.

The goal of the present study was to assess the ability of probiotic cocktail VSL#3 to alter the colonic microbiota and decrease inflammation-associated cancer when administered as interventional therapy. We report that therapeutic administration of VSL#3 probiotic did not protect against the development of colitis-associated CRC or inflammation in AOM/*Il10*$^{-/-}$ mice. In fact, we observed increased tumorigenesis in one of two cohorts of VSL#3-fed mice, relative to VSL#3-untreated mice. Illumina sequencing of this microbiota revealed that microbial community composition of the stool and mucosally-adherent compartments were significantly altered by VSL#3 administration. Depletion of a bacterial taxon assigned to genus *Clostridium* from the mucosally-adherent microbiota was identified as a mediator of VSL#3-enhanced tumorigenesis in this cohort. Together these findings demonstrate that therapeutic administration of VSL#3 does not protect against tumorigenesis in AOM/*Il10*$^{-/-}$ mice and may promote the loss of potentially protective microorganisms from the mucosally-adherent microbiota.

Results

VSL#3 does not protect against tumorigenesis in the AOM/*Il10*$^{-/-}$ model of colitis-associated CRC. To investigate the impact of probiotic intervention on development of colitis-associated CRC, we conventionalized germ-free (GF) *Il10*$^{-/-}$ mice with specific pathogen free (SPF) microbiota for seven weeks to establish intestinal inflammation. Conventionalizing mice born and raised in GF conditions negates the confounding factor of familial transmission of the microbiota. Tumorigenesis was then initiated with 6 weekly i.p. injections of AOM (10 mg/kg), at which point daily oral administration of VSL#3 (10^9 CFU/animal/day) was begun (Fig. 1).

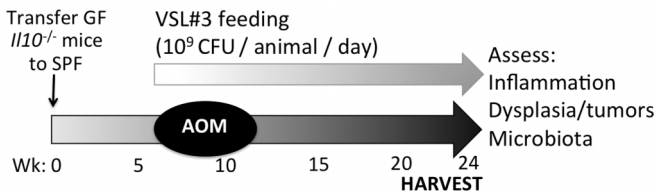

Figure 1 | Experimental timeline for AOM/*Il10*$^{-/-}$ model with VSL#3 interventional administration. Germ-free *Il10*$^{-/-}$ mice were transferred to SPF conditions where they were colonized with SPF commensal bacteria for seven weeks. Tumorigenesis was then initiated with six weekly injections of AOM (10 mg/kg), and VSL#3 was orally administered (10^9 CFU/mouse/day) to mice daily throughout the remainder of the experiment. After twenty-four weeks, mice were sacrificed and tissues were harvested for assessment of microbiota, inflammation, and tumorigenesis.

Based on previous reports showing that preventive administration of VSL#3 can reduce dysplasia and tumorigenesis in experimental models of inflammation-associated CRC[30,32], we hypothesized that interventional treatment would reduce tumorigenesis in the AOM/*Il10*$^{-/-}$ model. However, macroscopic assessment of tumor penetrance revealed no significant effect of VSL#3 on tumorigenesis, assessed seventeen weeks after the initial AOM injection (Fig. 2a). Microscopic scoring of neoplasia revealed high-grade dysplasia in 18/19 mice, with no significant difference in dysplasia score between VSL#3-treated and VSL#3-untreated animals (Fig. 2b). There was a potential trend towards greater depth of tumor invasion in VSL#3-treated animals that did not reach significance (Fig. 2c, chi-squared test $p = 0.095$).

To gain a better insight into VSL#3 effects on colitis-associated CRC in respect to microbial composition, we repeated the experiment using a second cohort of *Il10*$^{-/-}$ mice. Seventeen weeks after the initiation of tumorigenesis with AOM, miniature endoscopy of live anesthetized mice revealed large macroscopic lesions in VSL#3-treated animals that were rarely seen in VSL#3-untreated animals (Fig. 3a). Macroscopic examination of harvested colon tissue revealed that VSL#3-treatment induced visible tumors in 91% of mice, a significantly greater amount than the 38% observed in VSL#3-untreated mice that developed macroscopic lesions (Fig. 3b, c). Tumor multiplicity was also significantly enhanced by VSL#3,

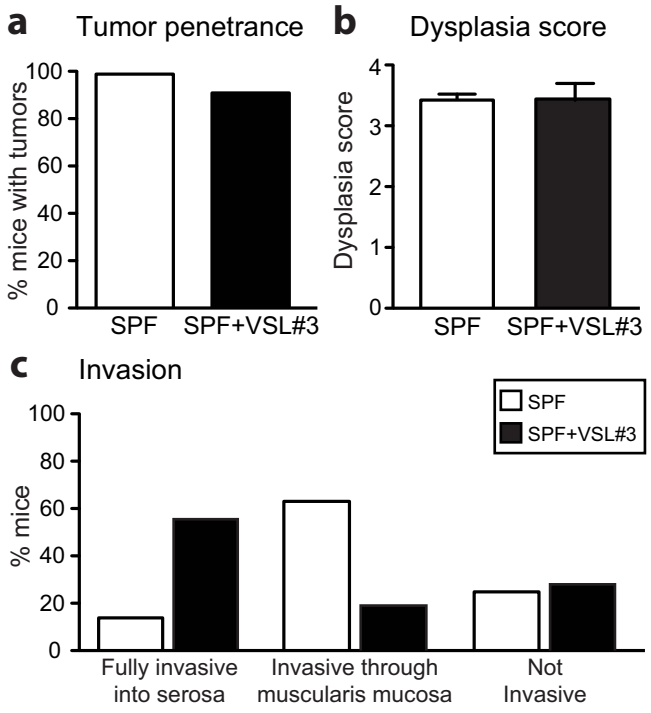

Figure 2 | VSL#3 does not affect tumorigenesis in AOM *Il10*$^{-/-}$ mice. (a) Tumor penetrance, non-significant by one sample t test comparing SPF + VSL#3 group to SPF control at 100%, $p = 0.341$ (b) dysplasia score, non-significant by two-tailed Mann Whitney U test, $p = 0.315$. Bar graphs (a–b) depict mean + SEM. (c) Tumor invasion, comparisons by chi-squared test, $p = 0.095$. (a–c) SPF $n = 8$, SPF + VSL#3 $n = 11$.

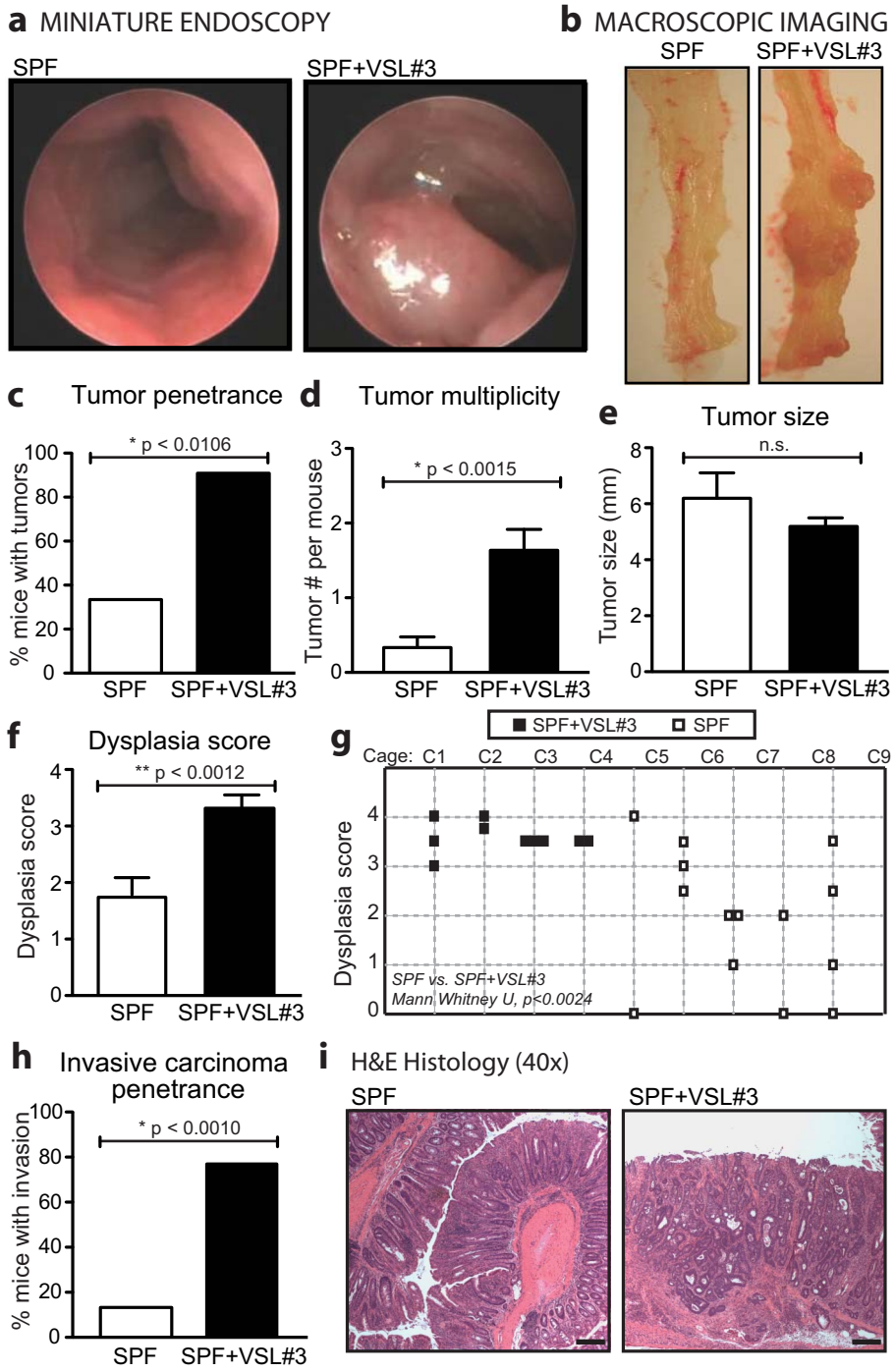

Figure 3 | VSL#3 enhances tumorigenesis in a second cohort of AOM *Il10*$^{-/-}$ mice. (a) Miniature endoscopy, (b) macroscopic imaging, (c) tumor penetrance, (d) tumor multiplicity, (e) dysplasia score, (f) individual dysplasia scores from the mice used for later microbiome (g) invasive adenocarcinoma penetrance, (h) representative H&E histology. (a–e, g) Bar graphs depict mean + SEM, 13–14 mice/group, pairwise comparisons by two-tailed Mann Whitney U test.

with an average of 1.64 macroscopic tumors per mouse vs. 0.33 tumors per mouse in VSL#3-untreated animals (Fig. 3d). Tumor size, however, remained unaffected by VSL#3 treatment (Fig. 3e). Histologic analysis of colonic sections revealed a significantly enhanced dysplasia score in VSL#3-treated animals (Fig. 3f). As observed in the first cohort, the cancer in VSL#3-fed animals was highly penetrant, with nearly all animals exhibiting advanced neoplasia (Fig. 3g). The majority of the VSL#3-fed mice harbored invasive adenocarcinomas (79% of mice), in contrast to only 13% of VSL#3-untreated mice (Fig. 3h, i). These results indicate that interventional treatment with VSL#3 does not protect against, and has the ability to enhance, tumorigenesis and tumor invasion in the AOM/*Il10*$^{-/-}$ model of colitis-associated CRC.

VSL#3 treatment does not impact colonic inflammation in the AOM/*Il10*$^{-/-}$ model. Chronic inflammation has been recognized as an important risk factor for CRC. We next assessed histologic inflammation in the distal and proximal colon of our second cohort of AOM/*Il10*$^{-/-}$ mice treated with or without VSL#3. We observed no significant difference in inflammation scores (Fig. 4a,

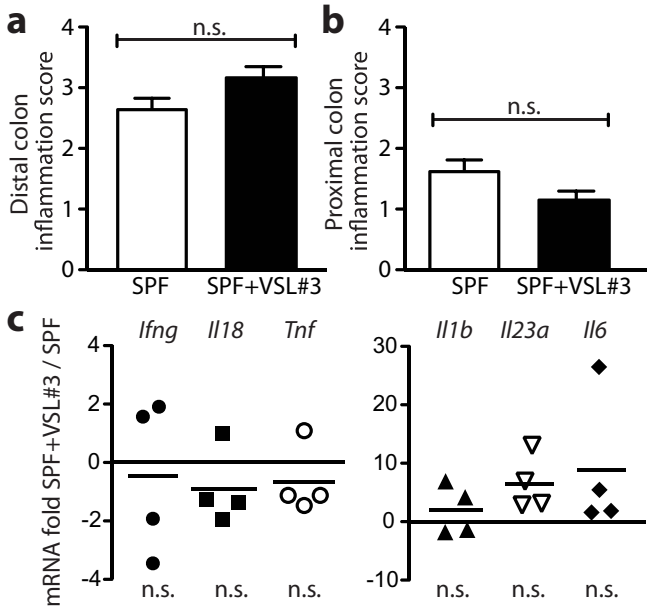

Figure 4 | VSL#3 does not significantly impact inflammation in AOM/*Il10*$^{-/-}$ mice. (a) Distal, and (b) proximal colon histologic inflammation scores, mean + SEM, 13–14 mice/group, pairwise comparisons by two-tailed Student t test. (c) Colonic cytokine mRNA expression of four individual SPF + VSL#3 mice relative to mean expression of four mice in the SPF group; line at median. Data analysis was performed with SABioscience RT^2 Profiler PCR Array Data Analysis version 3.4 using the ΔΔCt method and two-tailed Student t test.

b), demonstrating that intervention with VSL#3 does not alter colonic inflammation. To gain greater insight into the inflammatory environment of the colon, we measured inflammatory cytokine mRNA in colon tissue biopsies using an Inflammation PCR Array. There were no significant differences in the expression of common IBD- and CRC-associated cytokines including *Ifng, Il18, Tnf, Il1b, Il23a*, and *Il6* (Fig. 4c). Together these results suggest that VSL#3 enhances tumorigenesis without augmenting host inflammatory status.

VSL#3 alters community composition of both the luminal/stool and mucosally-adherent microbiota. Previous studies indicate that IBD and CRC patients have a dysbiotic microbiota[6,9,10,12,13]. In addition, we have previously demonstrated a bloom of Enterobacteriaceae in AOM/*Il10*$^{-/-}$ mice[8]. To determine the extent to which VSL#3 alters the microbiota, we utilized Illumina HiSeq2000 high-throughput sequencing. We extracted DNA from stool samples to assess the luminal microbiota and from colon tissue biopsies to assess the mucosally-adherent microbiota and sequenced the hypervariable V6 region of the 16S rRNA gene[8]. We sequenced the luminal microbiota of all animals, and one representative animal per cage for the mucosally-adherent microbiota. We found that VSL#3 treatment altered both the luminal (ANOSIM R = 0.381, P = 0.032) and mucosally-adherent (ANOSIM R = 0.406, P = 0.024) microbiota (Figure 5a). As expected, the composition of the luminal compartment differed from that of the mucosally-adherent microbiota (ANOSIM R = 0.466, $P < 0.001$). Diversity of the luminal and mucosally-adherent microbiota (Figure 5b and c) were not significantly altered by VSL#3 treatment, although there was a trend toward lower diversity in the luminal microbiota of VSL#3-fed animals.

VSL#3 alters the abundance of specific bacterial taxa of the luminal/stool and mucosally-adherent microbiota. To gain greater insight

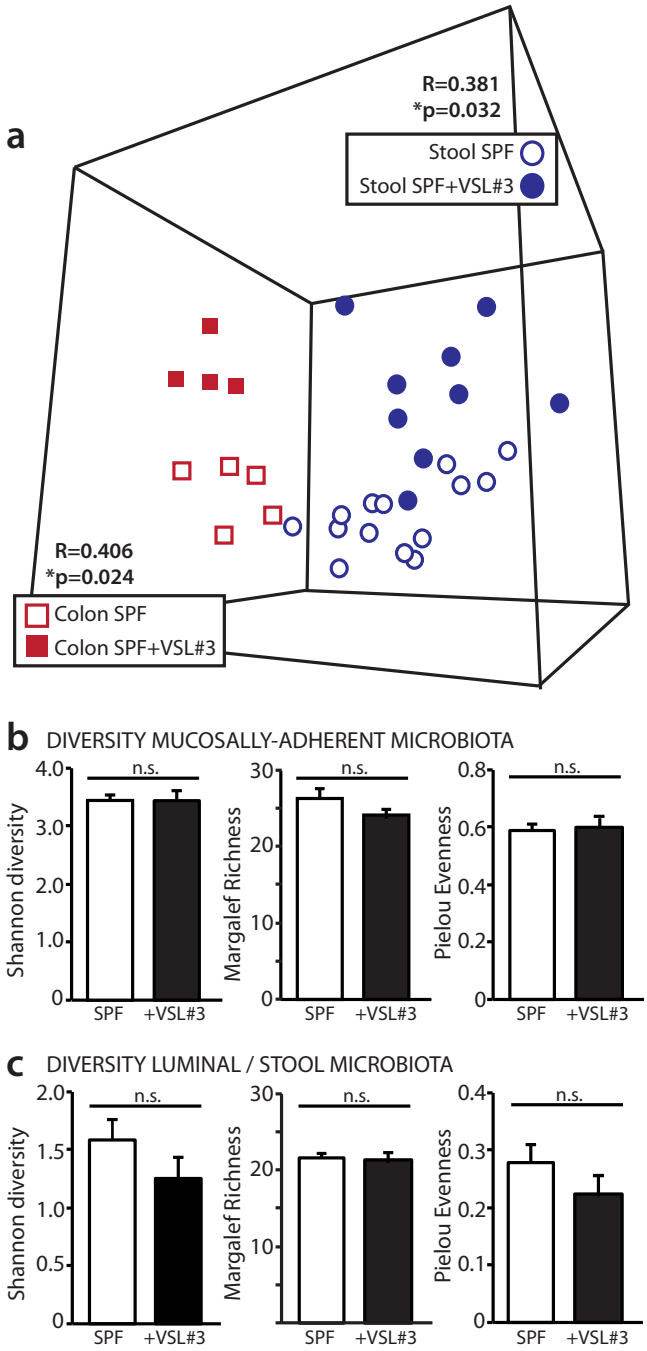

Figure 5 | VSL#3 (filled symbols) alters community composition of the luminal/stool (blue circles) and mucosally-adherent (red squares) microbiota. (a) Operational taxonomic unit (OTU) abundances were standardized by total, log-transformed, and assembled into a Bray Curtis similarity matrix to generate a multidimensional scaling (MDS) plot, where each symbol represents the microbiota of an individual mouse analyzed by Illumina sequencing of V6 16S. Analysis of similarity (ANOSIM) was used to test for dissimilarity between groups, where R = 1 is maximum dissimilarity. As expected, the luminal/stool microbiota differs from that of the mucosally-adherent microbiota, regardless of VSL#3 treatment (ANOSIM stool vs. adherent, R = 0.466, $P < 0.001$). (b–c) VSL#3 does not affect Shannon diversity, Margalef richness or Pielou evenness of the (b) mucosally-adherent or (c) luminal microbiota. Bar graphs depict the mean diversity, richness or evenness of (b) mean + SEM; SPF = 5 mice, SPF + VSL#3 = 4 mice, or (c) cage means + SEM (to correct for cage effects); SPF = 10 mice in 4 cages, SPF + VSL#3 = 14 mice in 5 cages. (b–c) Pairwise comparisons were made using Student t test.

into the microbial changes elicited by VSL#3 administration, we used BLASTn[36] to map the operational taxonomic unit (OTU) consensus sequences to the Silva database (http://www.arb-silva.de/) and classified the reference sequences using the RPD classifier[37]. In both the luminal/stool and mucosally-adherent compartments, VSL#3 administration altered the phylum-level distribution of the microbiota, with differences achieving significance at a false discovery rate (FDR) < 10% (Figure 6). VSL#3-treated animals exhibited a significant contraction of Verrucomicrobia and expansion of Proteobacteria in the mucosally-adherent microbiota. Within the luminal/stool microbiota, the abundance of Bacteroidetes was significantly decreased by VSL#3 treatment while Proteobacteria remained unaffected. To determine which specific microbial groups may be altered by VSL#3 treatment, we assessed the family-level distribution of the luminal/stool and mucosally-adherent microbiota. We were able to classify ~ 99% of reference sequences mapped to our OTUs to family level. At both the luminal/stool and mucosally-adherent compartments, VSL#3 treatment induced a contraction of Porphyromonadaceae and in the adherent compartment, also a contraction of Verrucomicrobiaceae (Figure 7). These changes were significant at $P < 0.05$ but not < 10% FDR, likely due to the large number of microbial families surveyed. Depletion, rather than expansion, of specific microbial groups in response to VSL#3 treatment suggests that a loss of protective microbes contributed to the significantly enhanced penetrance and severity of tumorigenesis in this model.

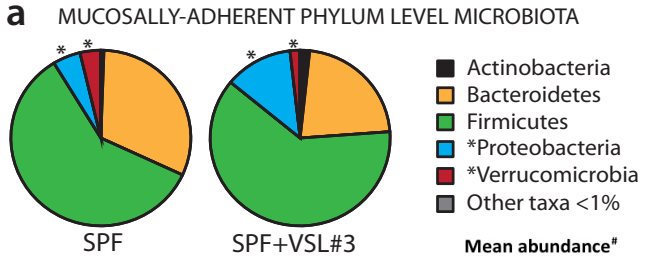

Phylum	p value	(n*p)/R	Mean abundance# SPF	SPF+VSL#3
*Verrucomicrobia	0.011	0.057	4.257	3.714
*Proteobacteria	0.023	0.059	4.272	4.651
Actinobacteria	0.070	0.117	3.349	3.787
Bacteroidetes	0.235	0.294	4.995	4.853
Firmicutes	0.634	0.634	5.280	5.303

*(n*p)/R are Benjamini Hotchberg false discovery rate corrected t test p values*
 # Raw abundance values were standardized to total and then log transformed

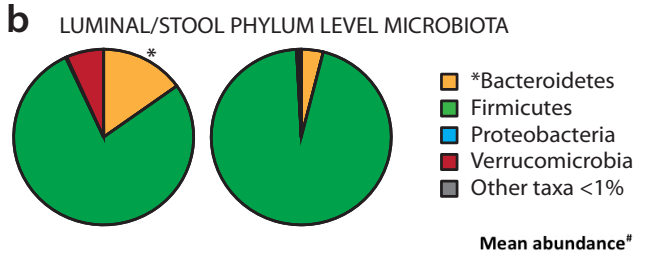

Phylum	p value	(n*p)/R	Mean abundance# SPF	SPF+VSL#3
*Bacteroidetes	0.024	0.095	4.684	4.178
Verrucomicrobia	0.067	0.134	4.356	3.937
Firmicutes	0.537	0.716	5.202	5.277
Proteobacteria	0.664	0.664	2.924	4.261

*(n*p)/R are Benjamini Hotchberg false discovery rate corrected mixed linear model p values*
 # Raw abundance values were standardized to total and then log transformed

Figure 6 | VSL#3 alters the phylum-level distribution of the (a) luminal/stool and (b) mucosally-adherent microbiota. Pie charts depict median standardized abundance (% of total) of the indicated phyla. (a) Standardized abundances of taxa contributing > 1% were log-transformed, pairwise comparisons were made using Student t test, and *P*-values were FDR corrected for multiple testing using the Benjamini and Hochberg procedure. SPF = 5 mice, SPF + VSL#3 = 4 mice. (b) Luminal/stool standardized log-transformed abundances were compared using a one way ANOVA by fitting a linear mixed model as described in Materials and Methods and *P*-values were corrected for multiple testing as in (a). SPF = 10 mice in 4 cages, SPF + VSL#3 = 14 mice in 5 cages.

Depletion of a *Clostridium* bacterial group is associated with VSL#3 administration and tumorigenesis. To determine if microbial alterations in the mucosally-adherent microbiota mediate the effects of VSL#3 on tumorigenesis, we performed mediation by linear models analysis[40] (Figure 8a and Methods section). In this analysis, we first tested the effect of VSL#3 on dysplasia (model 1). In agreement with earlier results presented in Figure 2, we found that VSL#3 was significantly associated with dysplasia score ($P < 0.0008$). We next applied model 2 to test the association of the relative abundance of all OTUs of the mucosally-adherent microbiota with dysplasia. We found that only a single taxon of the mucosal niche, OTU#199, had a significant association with dysplasia score (Benjamini and Hotchberg FDR corrected p = 0.0518). The consensus sequence of OTU#199 has an exact match to 38 distinct *Clostridium* taxa in the Silva database, and all of these full-length sequences were classified as Clostridiaceae I by RDP with a confidence score of 99% and *Clostridium* sensu stricto with a confidence score of 52%.

We next applied model 3, which indicated that VSL#3 treatment was associated with a significant (~16 fold) decrease in the relative abundance of OTU#199 (FDR corrected $P = 0.0525$; Figure 8b). Although the relative abundance of one other OTU of the mucosally-adherent microbiota was reduced in VSL#3 treated mice (FDR corrected p = 0.00073), model 2 analysis revealed that this OTU (best classified as *Blautia* sp., accession GQ493997.1.1354) was not associated with dysplasia (FDR corrected p > 0.10). From these combined results, we concluded that depletion of a mucosally-adherent *Clostridium* group was a potential mediator of the effects of VSL#3 on dysplasia/tumorigenesis.

To further evaluate this possibility, we applied model 4. We tested the effect of VSL#3 on dysplasia score without the influence of OTU#199, and found a high *P*-value (0.9399), which indicates that VSL#3 treatment is not directly associated with dysplasia. In contrast, when we tested the effect of OTU#199 on dysplasia score without the influence of VSL#3, we found a low *P*-value (FDR corrected $P = 0.0692$), supporting that the abundance of OTU#199 is associated with dysplasia. Taken together, the combined results of this mediation analysis by linear models indicated that depletion of OTU #199, a bacterial group of the genus *Clostridium*, is a potential mediator of the effects of VSL#3 on dysplasia/tumorigenesis in our experiment. These results demonstrate that VSL#3 may enhance dysplasia/tumorigenesis through depletion of *Clostridium* bacteria (OTU#199) at the mucosal niche.

Discussion

Intake of probiotics as a means to maintain health and alleviate disease symptoms, especially gastrointestinal disorders, has gained tremendous popularity worldwide. Although some of the beneficial impacts of probiotics have been scientifically documented, mechanisms of action and impact on established disease remained unclear. Introduction of billions of bacteria in a confined ecosystem such as the intestine is likely to impact the microbial community. Earlier work employing molecular fingerprinting analyses, including terminal restriction fragment length polymorphism (TRFLP) and denaturing gradient gel electrophoresis (DGGE), have revealed that administration of VSL#3 probiotic can alter microbial community composition of mice and rats[23,29,43,44]. To better understand the impact of interventional VSL#3 administration on the microbial community during development of colitis-associated CRC, we utilized high throughput Illumina 16S sequencing of the intestinal

a MUCOSALLY-ADHERENT FAMILY LEVEL MICROBIOTA

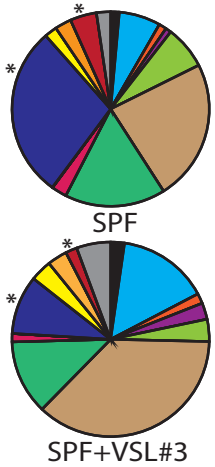

Family	p value	(n*p)/R	Mean abundance# SPF	SPF+VSL#3
*Verrucomicrobiaceae	0.015	0.193	4.250	3.727
*Porphyromonadaceae	0.021	0.134	4.864	4.420
Enterobacteriaceae	0.077	0.333	3.554	4.357
Lactobacillaceae	0.086	0.278	4.722	4.562
Chitinophagaceae	0.207	0.537	4.359	4.633
Pseudomonadaceae	0.216	0.467	3.784	4.038
Clostridiaceae.1	0.258	0.479	3.458	3.669
Burkholderiaceae	0.381	0.619	3.564	3.806
Lachnospiraceae	0.494	0.713	4.953	5.052
Ruminococcaceae	0.531	0.690	3.865	3.982
Peptostreptococcaceae	0.677	0.800	4.030	3.692
Erysipelotrichaceae	0.687	0.744	4.242	4.132
Planococcaceae	0.737	0.737	2.301	4.070
Other taxa <1%				

*(n*p)/R are Benjamini Hotchberg false discovery rate corrected t test p values*
 # Raw abundance values were standardized to total and then log transformed

b LUMINAL/STOOL FAMILY LEVEL MICROBIOTA

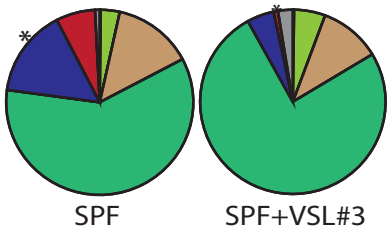

Family	p value	(n*p)/R	Mean abundance# SPF	+VSL#3
*Porphyromonadaceae	0.023	0.137	4.681	4.163
Verrucomicrobiaceae	0.068	0.203	4.355	3.931
Lachnospiraceae	0.392	0.784	4.427	4.636
Enterobacteriaceae	0.584	0.876	2.907	4.275
Lactobacillaceae	0.690	0.828	5.077	5.113
Erysipelotrichaceae	0.778	0.778	3.835	3.965
Other taxa <1%				

*(n*p)/R are Benjamini Hotchberg false discovery rate corrected mixed linear model p values*
 # Raw abundance values were standardized to total and then log transformed

Figure 7 | VSL#3 alters the family-level distribution of the (a) luminal/stool and (b) mucosally-adherent microbiota. Pie charts depict median standardized abundance (% of total) of the indicated phyla. (a) Standardized abundances of taxa contributing > 1% were log-transformed, pairwise comparisons were made using Student t test, and *P*-values were FDR corrected using the Benjamini and Hochberg procedure. SPF = 5 mice, SPF + VSL#3 = 4 mice. (b) Luminal/stool standardized log-transformed abundances were compared using a one way ANOVA by fitting a linear mixed model as described in Materials and Methods and *P*-values were corrected for multiple testing as in (a). SPF = 10 mice in 4 cages, SPF + VSL#3 = 14 mice in 5 cages.

microbiota of AOM/*Il10*$^{-/-}$ mice. Interventional administration of VSL#3 altered the composition of the luminal and mucosally-adherent microbiota with phylum level changes in the luminal microbiota (decrease in Bacteroidetes) and mucosally-adherent microbiota (decrease in Verrucomicrobia and increase in Proteobacteria). Depletion of specific bacterial groups at the family level, with Verrucomicrobiaceae in the adherent compartment and Porphyromonadaceae in the luminal and adherent compartments, was observed in VSL#3-exposed mice. Although we detected a non-significant increase in the abundance of VSL#3 bacterial groups Firmicutes and Lactobacillaceae, the major differences were detected in non-VSL#3 bacterial groups, indicating that administration of VSL#3 can exert pressure to induce broad changes in the microbial population of the intestine. These findings clearly demonstrate that VSL#3 administration markedly changed the composition of both the luminal and mucosally-associated microbiota.

An unexpected consequence of interventional administration of VSL#3 probiotic was the lack of a protective effect on tumorigenesis and the propensity to enhance tumor invasion in AOM/*Il10*$^{-/-}$ mice. We have previously demonstrated that inflammation in *Il10*$^{-/-}$ mice alters the composition of the intestinal microbiota with expansion of Proteobacteria, and this impacts the development of CRC[8]. In the current study, VSL#3 was therapeutically administered after the onset of inflammation and in the context of a dysbiotic microbiota. In contrast to other studies where prophylactic VSL#3 administration ameliorated colitis and colitis-associated CRC[24,29,30,32,45], our results have demonstrated that administration of VSL#3 beginning after the onset of inflammation and dysbiosis can enhance tumorigenesis. This was not associated with changes in inflammation or inflammatory cytokine profiles. Instead, enhanced tumorigenesis was associated with shifts in the composition of the intestinal microbiota in both the luminal/stool and mucosal niches. The initial composition of the microbial community likely influences probiotic effects on the host, as we also observed that prophylactic administration of VSL#3 beginning 3 days after transfer of *Il10*$^{-/-}$ mice from germ-free to SPF housing did not ameliorate inflammation nor early dysplasia (data not shown). In fact, we observed unexpected mortality in this treatment group, and terminated the experiment early at fourteen weeks post-transfer to SPF, six weeks after beginning AOM treatment (SPF vs. prophylactic VSL#3, log rank test $p = 0.040$). Altogether, these results suggest that probiotics may be ineffective and even detrimental to host health in the context of an immature or dysbiotic microbiota.

It also appeared that administration of VSL#3 predominantly induced depletion of bacterial groups, suggesting that tumorigenesis was enhanced through the loss of protective commensal bacteria. To determine if specific bacterial groups (classified into OTUs of 97% similarity) of the mucosally-adherent microbiota mediated the

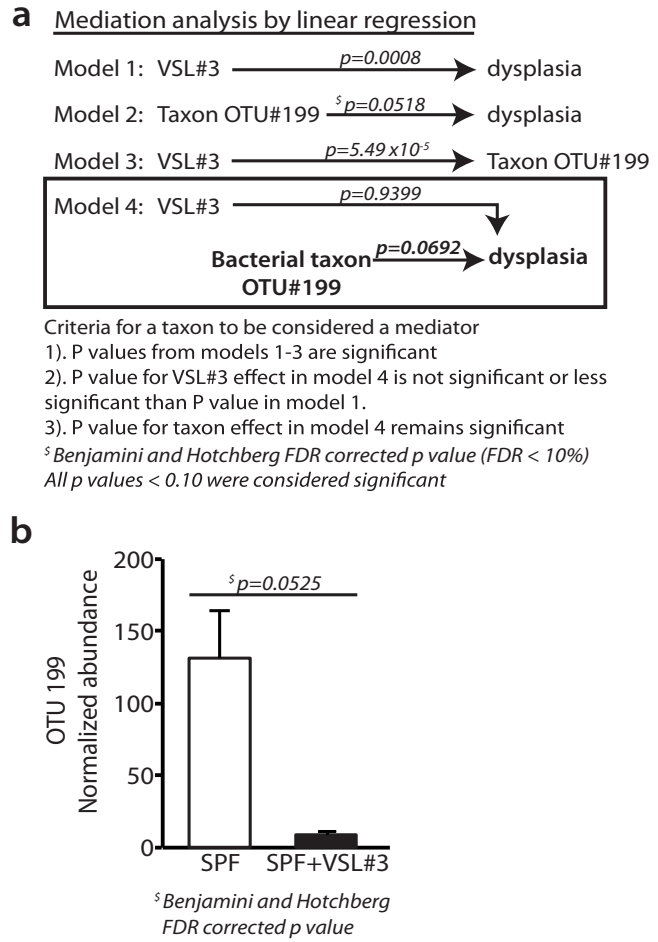

Figure 8 | Depletion of mucosally-adherent *Clostridium* bacteria mediates the effects of VSL#3 on dysplasia/tumorigenesis. (a) Mediation analysis by linear models was performed between VSL#3 status, dysplasia score, and each OTU in the stool or mucosally-adherent microbiota. Results for OTU #199 are shown. $P < 0.10$ was used as cutoff. The Benjamini and Hotchberg FDR adjustment was applied for multiple testing correction (model 2). A detailed description of the models is provided in Materials and Methods. (b) OTU #199, assigned to genus *Clostridium*, median log-normalized abundance + SEM. FDR-corrected *P*-value is shown, uncorrected *P*-value = 0.0002. SPF n = 5, SPF + VSL#3 n = 4.

effects of VSL#3 administration on tumorigenesis, we utilized a statistical approach termed mediation by linear models[40]. This approach first revealed that at a FDR corrected cutoff of $P < 0.1$, only one OTU of the mucosally-adherent microbiota, belonging to genus *Clostridium*, was a potential mediator of VSL#3 effects on tumorigenesis in our model. *Clostridium* sensu stricto, the sub-genus to which RDP classified this OTU with 52% confidence, is the largest sub-genus of *Clostridium* and comprises approximately 73 species[46–48]. Several of these species matched the consensus sequence of OTU#199 at 100% identity in the Silva database. *Clostridium* species have recently been shown to provide protection by inducing IL-10-producing intestinal T-regulatory cells, however, this trait is mainly attributed to Clostridium cluster IV and XIVa[49]. A major mechanism by which T-regulatory cells maintain homeostasis in the intestine is through the production of IL-10[50,51]. This protective mechanism is not intact in *Il10*$^{-/-}$ mice, thus it is unlikely that depletion of IL-10-producing T-regulatory cells is responsible for enhanced tumorigenesis in VSL#3-treated AOM/*Il10*$^{-/-}$ mice. An IL-10-independent mechanism of protection in the intestine is consistent with early work in which colitis was prevented in *Il10*$^{-/-}$ mice by prophylactic administration of VSL#3, which was associated with an enhancement of epithelial barrier function[24]. At this time, the impact of VSL#3 and depletion of Clostridium species on epithelial barrier function in our colitis-associated CRC model is unknown. In addition, future studies will be necessary to determine if VSL#3 induces the depletion of Clostridium species in other CRC models and in the absence of disease in healthy WT mice. Many Clostridium can ferment dietary fiber and host mucins to produce short chain fatty acids such as butyrate. Butyrate serves as a primary energy source for healthy colonocytes and regulates gene expression, inflammation, differentiation, and apoptosis in the intestine[52–54]. Butyrate and butyrate-producing bacteria have anti-inflammatory and anti-carcinogenic activities[55–58], and butyrate-producing bacteria are depleted in human IBD and CRC[6,59,60]. Thus depletion of *Clostridium* OTU#199 from the mucosally-adherent microbiota may reduce the production of butyrate and its anti-carcinogenic effects, resulting in enhanced tumorigenesis in AOM/*Il10*$^{-/-}$ mice. Butyrate and other short chain fatty acids are notoriously difficult to measure *in vivo*[61], however, if this hypothesis is correct, restoring the availability of butyrate in the intestine via prebiotic and/or novel probiotic supplementation with *Clostridium* could reveal a novel means by which to protect against IBD and CRC. Future studies will be necessary to determine if supplementation with any of the numerous bacteria represented by OTU#199 can promote protection or prevent VSL#3-induced enhancement of tumorigenesis in the AOM/*Il10*$^{-/-}$ model.

Together, our findings highlight several important concepts. First, probiotic bacteria may fail to protect against tumorigenesis in an environment with established dysbiosis. Earlier studies have revealed that VSL#3 probiotic can provide protection against colitis and colitis-associated CRC when VSL#3 is administered prior to the onset of inflammation[24,25,29,30,32,43,62]. VSL#3 bacteria can mediate protection in part through induction of IL-10[63], which is absent in our system and also in a subset of human IBD patients[64–66]. Thus it is possible that IL-10-independent effects of VSL#3 administration are not sufficient to overcome the pro-inflammatory and pro-carcinogenic effects of established dysbiosis in the AOM/*Il10*$^{-/-}$ model. Second, probiotic bacteria can alter the composition of the luminal and mucosally-adherent microbiota and induce the depletion of endogenous beneficial microbes at the mucosal niche. In the current study, we observed a detrimental effect that was potentially mediated by the loss of *Clostridium* bacteria. Given the complexity in the microbiota, it is not surprising to find evidence that certain bacteria may protect against inflammation while others protect against the progression of neoplasia. Undoubtedly, greater accessibility of new 'omics technologies will allow for a better understanding of the tremendous metabolic capacity of the microbiota and how microbial activities can be modulated to promote health and protect against disease.

Methods

AOM/*Il10*$^{-/-}$ model and probiotic administration. *Il10*-deficient 129/SvEv mice were born and raised in germ-free (GF) isolators and then transferred directly to our specific pathogen free (SPF) facility (age 7–12 weeks, housed 2–4 mice per cage) for the immediate initiation of our colitis/colorectal cancer experiment (Fig. 1). In this model, mice naturally acquire the microbiota from their cage/room microenvironment. This method of conventionalization negates any confounding familial or maternal transmission of the microbiota. We have recently characterized the microbiota of this model[38]. After 7 weeks of colonization with SPF bacteria, mice received 6 weekly i.p. injections of azoxymethane (AOM, 10 mg/kg). On the day of the first AOM injection, one group of mice was orally administered VSL#3 probiotic (Sigma-Tau Pharmaceuticals, Inc.), 10^9 CFU per animal each day during the week, with two days off on weekends, until the end of the experiment. The second group was not administered VSL#3 probiotic. After 17 weeks (24 weeks post-transfer from GF housing), miniature endoscopy was performed to visualize tumor development in live mice[31]. Mice were sacrificed, stool and tissue were collected, and colons were examined macroscopically for tumors then swiss-rolled and fixed in formalin for paraffin embedding and histology[31]. Histology was scored for inflammation[33] and dysplasia/tumors[8] by two blinded experienced investigators and reviewed by an

expert animal histopathologist. Dysplasia scoring was as follows: 0 = no dysplasia; 1 = mild dysplasia characterized by aberrant crypt doci (ACF), +0.5 for multiples; 2 = gastrointestinal neoplasia (GIN), +0.5 for multiples; 3 = adenoma, non-invasive severe or high grade dysplasia restricted to the mucosa; 3.5 = adenocarcinoma, invasive through the muscularis mucosa; 4 = adenocarcinoma, fully invasive through the submucosa and into or through the muscularis propria. Two independent experiments were conducted and data from both experiments are presented and discussed. All animal protocols were approved by the Institutional Animal Care and Use Committee of the University of North Carolina at Chapel Hill.

DNA extraction. Stool samples and mucosal biopsies were collected to assess luminal and mucosally-adherent microbiota respectively. Colon biopsies (2 × 10 mm) were collected after flushing the colon with PBS. Samples were immediately stored at −80°C. DNA was extracted from between 50–200 mg of stool or 100 mg colon tissue as described[8].

Illumina V6 16S library construction. The V6 hypervariable region of the 16S rRNA gene was amplified using a two-step PCR strategy[8]. The first step uses primers to the V6 region of the 16S gene that contain a 4–6 nucleotide barcode for multiplexing. The subsequent PCR adds Illumina paired-end sequencing adapters and a flow-cell adapter on the 5′ and 3′ ends of the amplicon. Amplicons were visualized on 1.5% agarose gel and purified using the QIAquick PCR purification kit (Qiagen). 50 ng of DNA from each sample was pooled to a final concentration of 29 ng/ul and subjected to paired-end Illumina HiSeq2000 sequencing at the University of North Carolina High Throughput Sequencing Facility.

Illumina sequencing. A single lane of Illumina HiSeq2000 generated 57,184,070 paired end sequences (144 multiplexed samples, 33 for this study) with a read length of ~ 75 bases, excluding primer sequences. Raw sequences were processed as described[8] except that we required at least 70 continuous matching nucleotides across the length of the ungapped alignment to generate each consensus sequence. A total of 39,537,745 paired-end sequences met our merging and extending criteria for the whole lane and 8,532,581 sequences belonged to the current study. Those 8,532,581 consensus sequences were fed in three batches into the program AbundantOTU v.2.0 (http://omics.informatics.indiana.edu/AbundantOTU/) with default parameters[34]. The first batch represented all 33 samples, the second represented only luminal/stool (LS) samples (24 samples, 5,568,718 consensus sequences) and the third represented mucosally-adherent (MA) samples (9 samples, 2,963,863 consensus sequences). AbundantOTU clustered these sequences into 1,064 (all), 439 (LS) and 857 (MA) Operational Taxonomic Units (OTUs). AbundantOTU incorporated 8,512,390 (99.76%) of all consensus sequences, 5,548,738 (99.64%) of the LS samples and 2,957,301 (99.78%) of the MA samples. The sequences that were not incorporated into an OTU were excluded from further analyses. A UCHIME v. 4.2.40 (http://www.drive5.com/uchime/[35]) search using the Gold reference database was used to detect the presence of chimeras in our OTUs. UCHIME reported 6 (all), 3 (LS) and 2 (MA) chimeras representing a negligible fraction of the total consensus sequences that were incorporated into OTUs. All reported chimeras were excluded from further analyses.

To facilitate taxonomic classification and to compensate for the short read length of the generated OTUs, we used BLASTn (v. 2.2.26+[36]) with an expectation value threshold of e-5 to map the OTU sequences to the Silva database (release 108, http://www.arb-silva.de/). Next, we utilized the standalone version of the RDP classifier (v. 2.5[37]) to classify the full-length Silva sequences with the best BLASTn match to the OTU sequence requiring an RDP confidence score of ≥ 80%.

Given the short read length of our Illumina V6 amplicon (~75 basepairs), we were unable to rigorously classify all OTUs, including #199, to species. In the Silva database, there were 38 full-length 16S sequences with an exact match to the consensus sequence of OTU #199. All were classified to genus Clostridium. RDP classified the consensus sequence for OTU#199 as Clostridiaceae I with 99% confidence and the sub-genus *Clostridium* sensu stricto with 52% confidence. Longer amplicons will be required to narrow this taxonomic assignment in future work.

Statistics. Statistical tests are described in figure legends and were computed using PRIMER v. 6, Microsoft Excel, Graphpad Prism, R v. 2.15.1 (http://www.R-project.org), and/or SAS v. 9.2 (SAS Institute Inc., Cary, NC). All tests are two-tailed, alpha = 0.05.

For microbiota analyses, OTU abundances were standardized to relative abundance, log-transformed, and analyzed with a Bray-Curtis similarity matrix using PRIMER v. 6 (PRIMERe, Inc). Analysis of Similarity (ANOSIM) was used to test for dissimilarity in community composition, and ordination plots were generated by multidimensional scaling (MDS). ANOSIM was nested on cage for the luminal microbiota; cage was not a factor for the mucosally-adherent microbiota as we assessed just one representative animal per cage. Before performing ANOSIM, we removed OTUs represented in < 25% of samples. Diversity was assessed by calculating Shannon diversity index, Margalef richness index and Pielou evenness index. For calculation of *P*-values for diversity in the luminal microbiota, the mean from all mice within a cage was utilized as an observational replicate. To compare the abundance of individual taxa between groups, we performed pairwise comparisons within the mucosally-adherent microbiota by t test and in the luminal/stool microbiota by fitting a mixed effect linear model of the form: $T = i + c_1V + c_2\,G(V) + e$ where T represents the Log Normalized Count; V represents treatment (VSL#3 or non-VSL#3); G represents the Cage; i is the intercept; c_1 and c_2 are coefficients for independent variables; e is the residual. This model takes into account the fact that multiple cages are involved and could contribute to the variation detected between samples[38]. VSL#3 was treated as a fixed effect while cage *nested* within VSL#3, the term G(V) in the model, was considered a random effect. All *P*-values were corrected for multiple testing using the Benjamini and Hochberg procedure[39] ($(n^*p)/R$ where n = # taxa, p = test *P*-value, R = rank by raw *P*-value) at a false discovery rate (FDR) threshold of 10%. Before performing pairwise comparisons, we excluded low abundance taxa that contributed < 1%.

Baron & Kenny's four steps approach[40–42], the most widely used method to assess causal mediation, was used to evaluate each OTU in the mucosally-adherent microbiota for its potential mediation effect between VSL#3 and dysplasia. This analysis was performed through four linear models using SAS v. 9.2. Model 1 tests that VSL#3 is significantly associated with dysplasia score. Model 2 tests that the relative abundance of the OTU is significantly associated with dysplasia. Model 3 tests the VSL#3 effect on the relative abundance of the OTU (for OTUs found to have a significant effect on dysplasia in model 2). Model 4 tests whether the bacterial taxon (i.e. OTU#199) affects dysplasia without the influence of VSL#3, and whether VSL#3 affects dysplasia without the influence of OTU#199. Equations: Model 1, $D = i_1 + c_1V + e_1$; Model 2, $D = i_2 + c_2T + e_2$; Model 3, $T = i_3 + c_3V + e_3$; Model 4, $D = i_4 + c_4T + c_5V + e_4$. D represents dysplasia score; V represents treatment (VSL#3 or non-VSL#3); T represents the log-normalized relative abundance of a particular taxon (OTU); i_1, i_2, i_3, i_4 are intercepts; c_1, c_2, c_3, c_4, c_5 are coefficients for independent variables; e_1, e_2, e_3, e_4 are residuals.

OTUs were considered as potential mediators if they met the three criteria proposed by Baron & Kenny: (i) *P*-values from models 1–3 are significant, (ii) The *P*-value for the VSL#3 effect in model 4 is less significant than in model 1 and (iii) The *P*-value for the OTU relative abundance effect in model 4 remains significant. The Benjamini and Hotchberg procedure was applied for multiple comparisons and FDR-corrected $P < 0.10$ was considered significant. As all four models belong to one analysis, a single $P < 0.10$ cutoff was applied. Each taxon was tested separately for its mediation effect.

Inflammation PCR arrays. Inflammatory gene expression was evaluated using SABiosciences array as described by us[8]. Briefly, RNA was extracted from distal colon biopsies (4 per group) using phenol:chloroform, DNase treatment (Qiagen) and RNeasy kit (Qiagen). 1 μg of RNA was transcribed to cDNA using RT2 First Strand kit (Qiagen/SABiosciences). Expression of inflammatory mediators was assessed using inflammation array PAMM-077 (Qiagen/SABiosciences). Data analysis was performed with SABioscience RT2 Profiler PCR Array Data Analysis version 3.4 (Qiagen/SA Biosciences: http://pcrdataanalysis.sabiosciences.com/pcr/arrayanalysis.ph) using the ΔΔCt method after normalizing to five housekeeping genes. Data are presented as fold changes for four individual VSL#3-treated mice, relative to the mean of four SPF mice.

1. Klaenhammer, T. R., Kleerebezem, M., Kopp, M. V. & Rescigno, M. The impact of probiotics and prebiotics on the immune system. *Nat. Rev. Immunol.* **12**, 728–734 (2012).
2. Gareau, M. G., Sherman, P. M. & Walker, W. A. Probiotics and the gut microbiota in intestinal health and disease. *Nat Rev Gastroenterol Hepatol* **7**, 503–514 (2010).
3. Manichanh, C., Borruel, N., Casellas, F. & Guarner, F. The gut microbiota in IBD. *Nat Rev Gastroenterol Hepatol* **9**, 599–608 (2012).
4. Isaacs, K. & Herfarth, H. Role of probiotic therapy in IBD. *Inflamm. Bowel Dis.* **14**, 1597–1605 (2008).
5. Backhed, F., Ley, R. E., Sonnenburg, J. L., Peterson, D. A. & Gordon, J. I. Host-bacterial mutualism in the human intestine. *Science* **307**, 1915–1920 (2005).
6. Sokol, H., Lay, C., Seksik, P. & Tannock, G. W. Analysis of bacterial bowel communities of IBD patients: what has it revealed? *Inflamm. Bowel Dis.* **14**, 858–867 (2008).
7. Arthur, J. C. & Jobin, C. The struggle within: microbial influences on colorectal cancer. *Inflamm. Bowel Dis.* **17**, 396–409 (2011).
8. Arthur, J. C. *et al.* Intestinal Inflammation Targets Cancer-Inducing Activity of the Microbiota. *Science* **338**, 120–123 (2012).
9. Frank, D. N. *et al.* Molecular-phylogenetic characterization of microbial community imbalances in human inflammatory bowel diseases. *Proceedings of the National Academy of Sciences of the United States of America* **104**, 13780–13785 (2007).
10. Willing, B. P. *et al.* A pyrosequencing study in twins shows that gastrointestinal microbial profiles vary with inflammatory bowel disease phenotypes. *Gastroenterology* **139**, 1844–1854 e1 (2010).
11. Sobhani, I. *et al.* Microbial dysbiosis in colorectal cancer (CRC) patients. *PLoS ONE* **6**, e16393 (2011).
12. Sanapareddy, N. *et al.* Increased rectal microbial richness is associated with the presence of colorectal adenomas in humans. *ISME J* **6**, 1858–1868 (2012).
13. Shen, X. J. *et al.* Molecular characterization of mucosal adherent bacteria and associations with colorectal adenomas. *Gut Microbes* **1**, 138–147 (2010).
14. Jobin, C. Colorectal cancer: looking for answers in the microbiota. *Cancer Discov* **3**, 384–387 (2013).
15. Kostic, A. D. *et al.* Genomic analysis identifies association of Fusobacterium with colorectal carcinoma. *Genome Research* **22**, 292–298 (2011).
16. Swidsinski, A. *et al.* Association between intraepithelial Escherichia coli and colorectal cancer. *Gastroenterology* **115**, 281–286 (1998).

17. Martin, H. M. *et al.* Enhanced Escherichia coli adherence and invasion in Crohn's disease and colon cancer. *Gastroenterology* **127**, 80–93 (2004).
18. Darfeuille-Michaud, A. *et al.* Presence of adherent Escherichia coli strains in ileal mucosa of patients with Crohn's disease. *Gastroenterology* **115**, 1405–1413 (1998).
19. Garrett, W. S. *et al.* Enterobacteriaceae act in concert with the gut microbiota to induce spontaneous and maternally transmitted colitis. *Cell Host Microbe* **8**, 292–300 (2010).
20. Gionchetti, P. *et al.* Oral bacteriotherapy as maintenance treatment in patients with chronic pouchitis: a double-blind, placebo-controlled trial. *Gastroenterology* **119**, 305–309 (2000).
21. Gionchetti, P. *et al.* Prophylaxis of pouchitis onset with probiotic therapy: a double-blind, placebo-controlled trial. *Gastroenterology* **124**, 1202–1209 (2003).
22. Sood, A. *et al.* The probiotic preparation, VSL#3 induces remission in patients with mild-to-moderately active ulcerative colitis. *Clin Gastroenterol Hepatol* **7**, 1202–1209 (2009).
23. Bibiloni, R. *et al.* VSL#3 probiotic-mixture induces remission in patients with active ulcerative colitis. *Am. J. Gastroenterol.* **100**, 1539–1546 (2005).
24. Madsen, K. *et al.* Probiotic bacteria enhance murine and human intestinal epithelial barrier function. *Gastroenterology* **121**, 580–591 (2001).
25. Pagnini, C. *et al.* Probiotics promote gut health through stimulation of epithelial innate immunity. *Proceedings of the National Academy of Sciences of the United States of America* **107**, 454–459 (2010).
26. Gaudier, E., Michel, C., Segain, J.-P., Cherbut, C. & Hoebler, C. The VSL# 3 probiotic mixture modifies microflora but does not heal chronic dextran-sodium sulfate-induced colitis or reinforce the mucus barrier in mice. *J. Nutr.* **135**, 2753–2761 (2005).
27. Hörmannsperger, G. *et al.* Post-Translational Inhibition of IP-10 Secretion in IEC by Probiotic Bacteria: Impact on Chronic Inflammation. *PLoS ONE* **4**, e4365 (2009).
28. Shen, B. *et al.* Maintenance therapy with a probiotic in antibiotic-dependent pouchitis: experience in clinical practice. *Aliment. Pharmacol. Ther.* **22**, 721–728 (2005).
29. Bassaganya-Riera, J. *et al.* Probiotic bacteria produce conjugated linoleic acid locally in the gut that targets macrophage PPAR γ to suppress colitis. *PLoS ONE* **7**, e31238 (2012).
30. Bassaganya-Riera, J., Viladomiu, M., Pedragosa, M., De Simone, C. & Hontecillas, R. Immunoregulatory mechanisms underlying prevention of colitis-associated colorectal cancer by probiotic bacteria. *PLoS ONE* **7**, e34676 (2012).
31. Uronis, J. M. *et al.* Modulation of the intestinal microbiota alters colitis-associated colorectal cancer susceptibility. *PLoS ONE* **4**, e6026 (2009).
32. Appleyard, C. B. *et al.* Pretreatment with the probiotic VSL#3 delays transition from inflammation to dysplasia in a rat model of colitis-associated cancer. *Am J Physiol Gastrointest Liver Physiol* **301**, G1004–G1013 (2011).
33. Karrasch, T., Kim, J. S., Muhlbauer, M., Magness, S. T. & Jobin, C. Gnotobiotic IL-10-/-;NF-kappa B(EGFP) mice reveal the critical role of TLR/NF-kappa B signaling in commensal bacteria-induced colitis. *J. Immunol.* **178**, 6522–6532 (2007).
34. Ye, Y. 2010 IEEE International Conference on Bioinformatics and Biomedicine (BIBM). 153–157 (2010).
35. Edgar, R. C., Haas, B. J., Clemente, J. C., Quince, C. & Knight, R. UCHIME improves sensitivity and speed of chimera detection. *Bioinformatics* **27**, 2194–2200 (2011).
36. Altschul, S. Gapped BLAST and PSI-BLAST: a new generation of protein database search programs. *Nucleic Acids Research* **25**, 3389–3402 (1997).
37. Wang, Q., Garrity, G. M., Tiedje, J. M. & Cole, J. R. Naive Bayesian classifier for rapid assignment of rRNA sequences into the new bacterial taxonomy. *Appl Environ Microb* **73**, 5261–5267 (2007).
38. McCafferty, J. *et al.* Stochastic changes over time and not founder effects drive cage effects in microbial community assembly in a mouse model. *ISME J* (2013). doi:10.1038/ismej.2013.106
39. Benjamini, Y. & Hotchberg, Y. Controlling the false discover rate: a practical and powerful approach to multiple testing. *Journal of the Royal Statistical Society Series B* **57**, 289–300 (1995).
40. Baron, R. M. & Kenny, D. A. The moderator–mediator variable distinction in social psychological research: Conceptual, strategic, and statistical considerations. *Journal of Personality and Social Psychology* **51**, 1173–1182 (1986).
41. Kenny, D. A., Kashy, D. A. & Bolger, N. Data analysis in social psychology. In Gilbert, D., Fiske, S. & Lindzey, G. ed. *Handbook of Social Psychology.* 4th ed. New York: McGraw-Hill; 233–265 (1998).
42. MacKinnon, D. P., Fairchild, A. J. & Fritz, M. S. Mediation Analysis. *Annual review of psychology* **58**, 593–614 (2007).
43. Uronis, J. M. *et al.* Gut microbial diversity is reduced by the probiotic VSL#3 and correlates with decreased TNBS-induced colitis. *Inflamm. Bowel Dis.* **17**, 289–297 (2011).
44. Reiff, C. *et al.* Balancing inflammatory, lipid, and xenobiotic signaling pathways by VSL#3, a biotherapeutic agent, in the treatment of inflammatory bowel disease. *Inflamm. Bowel Dis.* **15**, 1721–1736 (2009).
45. Santiago, C., Pagan, B., Isidro, A. A. & Appleyard, C. B. Prolonged chronic inflammation progresses to dysplasia in a novel rat model of colitis-associated colon cancer. *Cancer Res.* **67**, 10766–10773 (2007).
46. Johnson, J. L. & FRANCIS, B. S. Taxonomy of the Clostridia: Ribosomal Ribonucleic Acid Homologies among the Species. *Journal of General Microbiology* **88**, 229–244 (1975).
47. Collins, M. D. *et al.* The Phylogeny of the Genus Clostridium: Proposal of Five New Genera and Eleven New Species Combinations. *International Journal of Systematic Bacteriology* **44**, 812–826 (1994).
48. Falkow, S., Rosenberg, E., Schleifer, K.-H. & Stackebrandt, E. An introduction to the family Costridiaceae. *The Prokaryotes Vol* **4**, 3rd ed. New York: Springer 654–677 (2006).
49. Atarashi, K. *et al.* Induction of colonic regulatory T cells by indigenous Clostridium species. *Science* **331**, 337–341 (2011).
50. Barnes, M. J. & Powrie, F. Regulatory T Cells Reinforce Intestinal Homeostasis. *Immunity* **31**, 401–411 (2009).
51. Rubtsov, Y. P. *et al.* Regulatory T Cell-Derived Interleukin-10 Limits Inflammation at Environmental Interfaces. *Immunity* **28**, 546–558 (2008).
52. Scheppach, W. Effects of short chain fatty acids on gut morphology and function. *Gut* **35**, S35–8 (1994).
53. Louis, P. & Flint, H. J. Diversity, metabolism and microbial ecology of butyrate-producing bacteria from the human large intestine. *FEMS Microbiology Letters* **294**, 1–8 (2009).
54. Hamer, H. M. *et al.* Review article: the role of butyrate on colonic function. *Aliment. Pharmacol. Ther.* **27**, 104–119 (2008).
55. Pajak, B. & Orzechowski, A. Molecular basis of sodium butyrate-dependent proapoptotic activity on cancer cells. *Adv Med Sci* **52**, 83–88 (2007).
56. Maslowski, K. M. *et al.* Regulation of inflammatory responses by gut microbiota and chemoattractant receptor GPR43. *Nature* **461**, 1282–1286 (2009).
57. Arimochi, H., Morita, K., Nakanishi, S., Kataoka, K. & Kuwahara, T. Production of apoptosis-inducing substances from soybean protein by Clostridium butyricum: characterization of their toxic effects on human colon carcinoma cells. *Cancer Lett.* **277**, 190–198 (2009).
58. Nakanishi, S., Kataoka, K., Kuwahara, T. & Ohnishi, Y. Effects of high amylose maize starch and Clostridium butyricum on metabolism in colonic microbiota and formation of azoxymethane-induced aberrant crypt foci in the rat colon. *Microbiol. Immunol.* **47**, 951–958 (2003).
59. Manichanh, C. *et al.* Reduced diversity of faecal microbiota in Crohn's disease revealed by a metagenomic approach. *Gut* **55**, 205–211 (2006).
60. Wang, T. *et al.* Structural segregation of gut microbiota between colorectal cancer patients and healthy volunteers. *ISME J* **6**, 320–329 (2011).
61. Aluwé, M., Delezie, E. & De Brabander, D. L. Prediction of In Vivo Short-Chain Fatty Acid Production in Hindgut Fermenting Mammals: Problems and Pitfalls. *Crit Rev Food Sci Nutr* **50**, 605–619 (2010).
62. Mennigen, R. *et al.* Probiotic mixture VSL#3 protects the epithelial barrier by maintaining tight junction protein expression and preventing apoptosis in a murine model of colitis. *Am J Physiol Gastrointest Liver Physiol* **296**, G1140–G1149 (2009).
63. Madsen, K. Probiotics and the immune response. *J. Clin. Gastroenterol.* **40**, 232–234 (2006).
64. Schlee, M. *et al.* Probiotic lactobacilli and VSL#3 induce enterocyte β-defensin 2. *Clinical & Experimental Immunology* **151**, 528–535 (2008).
65. Shah, N., Kammermeier, J., Elawad, M. & Glocker, E.-O. Interleukin-10 and Interleukin-10–Receptor Defects in Inflammatory Bowel Disease. *Curr Allergy Asthma Rep* **12**, 373–379 (2012).
66. Kotlarz, D. *et al.* Loss of interleukin-10 signaling and infantile inflammatory bowel disease: implications for diagnosis and therapy. *Gastroenterology* **143**, 347–355 (2012).

Acknowledgements

We thank M. Bower of the National Gnotobiotic Rodent Resource Center at University of North Carolina for assistance with gnotobiotic mice (NIH P40 R018603), and Brigitte Allard and Dana Marie Walsh for technical assistance. We thank Dr. Arlin Rogers for assistance with histological evaluation of colonic tumors. Histology was performed at the CGIBD histology core (P30 DK034987). This work was supported by funding from NIH T32 DK007737 (JCA), R01 DK73338 (CJ), R01 DK47700 (CJ), and the American Institute for Cancer Research (CJ).

Author contributions

J.C.A., J.M.U. and C.J. designed the study; J.C.A., R.Z.G., J.M.U., E.P.C., S.T. acquired data; J.C.A., R.Z.G., J.M.U., M.M., A.F. and C.J. analyzed and interpreted data; J.C.A., R.Z.G., W.S. and A.F. performed statistical analysis; J.C.A., R.Z.G., A.F. and C.J. wrote and revised the manuscript. All authors reviewed the manuscript.

Additional information

Accession codes: Reads were deposited in MGRAST under project ID 4965

Competing financial interests: The authors declare no competing financial interests.

How to cite this article: Arthur, J.C. *et al.* VSL#3 probiotic modifies mucosal microbial composition but does not reduce colitis-associated colorectal cancer. *Sci. Rep.* **3**, 2868; DOI:10.1038/srep02868 (2013).